http://ansinet.com/itj



ISSN 1812-5638

# INFORMATION TECHNOLOGY JOURNAL



Asian Network for Scientific Information 308 Lasani Town, Sargodha Road, Faisalabad - Pakistan

# Hybrid Segmentation Using Region Information for Wireless Capsule Endoscopy Image

Yihua Lan, Xingang Zhang, Zhidu Liu, Li Zhao and Ming Li School of Computer and Information Technology, Nanyang Normal University, Nanyang, 473061, China Department of Imaging Processing Business, Beijing E-COM Technology Co., Ltd., Beijing, 100176, China

Abstract: With the advantages of being painless, safe and easy-to-use, wireless capsule endoscopy has become a hot research topic in clinical medicine. As tens of thousands of images are generated during an examination, it is impractical for manual image checking. Utilizing computer image processing can greatly enhance image quality, decrease diagnosis time and improve diagnosis accuracy. One of the critical requirements of the employed image processing methods is to extract the lesion areas. Although, many image segmentation methods have been proposed, accurate image segmentation is also a challenging problem which is not completely solved yet. At present, those segmentation approaches can be divided into two main categories: Region based and edge based. It is often difficult to obtain satisfactory results when using only one of these methods in the segmentation of complex pictures. Therefore, in this study, a new image segmentation method using both region and edge information is proposed to combine the two types of methods or information to achieve accurate segmentation results. Experimental results demonstrate the efficacy of the proposed method.

Key words: Wireless capsule endoscopy, image segmentation, total variation model, region information

# INTRODUCTION

The invention of wireless capsule endoscopy is a breakthrough in the field of biomedical. It has become the hot topic in clinical medical research as well as recognized by clinical examination in practice. About 50,000 to 60,000 colored-images are generated in one examination, it is thus a heavy task to process huge amounts of image data, extract abnormal images and confirm the disease categories and their locations. To improve the efficiency of image examination, accuracy of diagnosis, it is crucial to develop computed-aided image processing techniques for wireless capsule endoscopy. One of the requirements in the image processing techniques is to efficiently perform image segmentation, automate the selection of abnormal information from large amounts of images, which can help extract and locate the lesion areas.

Many segmentation algorithms have been proposed. Those algorithms can be mainly classed into two categories: Region-based methods and edge based methods. The two types of methods have their advantages and disadvantages, respectively. The region based methods assign each pixel in the image being

classified to a particular region or object by using one or some predefined criteria. Many algorithms can be categorized to be this class, such as split-and-merge algorithms (Zhang et al., 2003) and region growing techniques. Region growing segmentation method is one of the most popular examples of this category (Adams and Bischof, 1994; Mendoza et al., 2012). For example, Rolf Adams and Leanne Bischof proposed a seeded region growing as applied to gray-scale images. There followed a number of other different approaches based on region growing technique, such as fuzzy region growing methods proposed by Guliato et al. (1998) and object region growing in combination with a density-weighted contrast enhancement filter proposed by Petrick et al. (1999). One of the main problems of region growing algorithms is that low-contrast or small structures are prone to grow into the background, which can be lead to large regions even though the actual object is quite small (Timp and Karssemeijer, 2004).

Different with the algorithms in the above category, the boundary of an object is detected in edge based methods. In this class of segmentation method, most of them first construct or provide an initial edge by using manual selection (Timp and Karssemeijer, 2004), each pixel in this edge is assigned a value according to some criteria such as the edge strength or else, then, whether or not those pixels or new pixels are selected which is evolved by automated procedures. At last, those ultimate selected pixels will be linkedto represent the final object boundaries. The main problem of this type of method is that a closed contour could not be guaranteed.

Due to the complicated lightning condition, the image is of low contrast which leads to poor outcomes of segmentation of current methods.

Comparing with traditional segmentation methods, Active Contour Models (ACM) model (Kass *et al.*, 1988), which combines level-set methods and curve evolution, is more suitable for processing diverse and complicate images and thus has broader usage.

In this study, on the basis of the analysis of the capsule image characteristics, we use a new ACM combines the imprecise region information and edge information by a Total Variation (TV) model to segment Region Of Interest (ROI) from capsule endoscopy images. The rest of this study is organized as follows: In section 2, we review the classic Geodesic Active Contour (GAC) (Caselles et al., 1997) and C-V (Chan and Vese, 2001) models, TV method. Section 3 describes the proposed total variation segmentation with imprecise region information methods. The numerical solution of the proposed model is also introduced in this section. Experimental results are shown in section 4. At last conclusions is given in the section 5.

## RLATED WORK

**GAC model:** GAC model can be defined via an energy functional (Caselles *et al.*, 1997):

$$\min_{C} \left\{ E_{GAC}(C) = \int_{0}^{L(C)} g(|\nabla I_{o}(C(s))|) ds \right\}$$
 (1)

where ds is the Euclidean element of Length and L  $\left(C\right)$  is the length of the curve C. The function g is an edge indicator function that vanishes at object boundaries, such as:

$$g(|\nabla I_o|) = \frac{1}{1 + \beta |\nabla I_o|^2}$$

or:

$$g(|\nabla I_{\alpha}|) = e^{-\eta |\nabla I_{\alpha}|^{3}}$$

where,  $I_0$  is the original image and  $\beta$ ,  $\eta$ ,  $\kappa$  are positive constants.

We can get an evolution equation based on variation principle and gradient descent method:

$$\partial_t C = \left(\kappa g - \left\langle \nabla g, \vec{N} \right\rangle \right) \vec{N} \tag{2}$$

where, t is an introduced parameter representing the evolution of curve with the change of time. While,  $\kappa$  and  $\bar{N}$  denote the curvature and normal vector separately. A constant  $\alpha$  is added to prevent curve collapse in smooth areas. Accordingly, the following evolution equation can be derived:

$$\partial_{t}C = \left( (\kappa + \alpha)g - \left\langle \nabla g, \overrightarrow{\mathbf{N}} \right\rangle \right) \overrightarrow{\mathbf{N}} \tag{3}$$

The corresponding level set expression is as follows:

$$\frac{\partial \phi}{\partial t} = g. \left( \text{div} \left( \frac{\nabla \phi}{|\nabla \phi|} \right) + \alpha \right) \! |\nabla \phi| + \nabla g \cdot \nabla \phi \tag{4} \right)$$

**C-V model:** C-V model is a simplified M-S model, with the following energy function (Chan and Vese, 2001):

$$\min_{\substack{C, c_1, c_2 \\ +\lambda_1 \int_{\text{inside}(C)} (\mathbf{I}(\mathbf{x}) - \mathbf{c}_1)^2 \, d\mathbf{x} \\ +\lambda_2 \int_{\text{outside}(C)} (\mathbf{I}(\mathbf{x}) - \mathbf{c}_2)^2 \, d\mathbf{x}}}$$

$$(5)$$

where  $\Omega$  is the image region,  $\lambda_1$ ,  $\lambda_2 > 0$  are the parameters.  $c_1$  and  $c_2$  represent respectively the average gray value inside and outside the contours changing with its evolution:

$$\min_{\substack{\phi, c_1, c_2 \\ \phi, c_1, c_2}} \left\{ E_{CV}(\phi, c_1, c_2) = \int_{\Omega} \left| \nabla H_{\varepsilon}(\phi) \right| + \int_{\Omega} \left( \lambda_1 H_{\varepsilon}(\phi) (I(\mathbf{x}) - c_1)^2 \right) d\mathbf{x} \right\}$$
(6)

Since, Heaviside is an ideal and non-differentiable function, it is always replaced by Heaviside ( $H_{\epsilon}$ ) after regularization. With calculation of variation, we can get the evolution equation of energy function as follows:

$$\frac{\partial \phi}{\partial t} = \mathbf{H}_{\varepsilon}^{'}(\phi) \left\{ \frac{\operatorname{div}\left(\frac{\nabla \phi}{|\nabla \phi|}\right) - \left(\lambda_{1} (\mathbf{I}(\mathbf{x}) - \mathbf{c}_{1})^{2} - \lambda_{2} (\mathbf{I}(\mathbf{x}) - \mathbf{c}_{2})^{2}\right) \right\}$$
(7)

**TV model:** Total Variation (TV) has been a landmark in the history of image processing. It is a classical application of Bounded Variation (BV) in this field. For a better

understanding of TV model, the conception of BV theory is briefly introduced as follows (Chan and Shen, 2002):

Suppose  $\Omega \in \mathbb{R}^2$  represents the image areas. For  $f \in L_{loc}^{-1}(\Omega)$ , the total variation can be defined as follows:

$$TV(f) = \int_{O} |\nabla f| dx = \int_{O} \sqrt{f_{x_1}^2 + f_{x_2}^2} dx_1 dx_2$$
 (8)

Accordingly, the definition of BV space is given as below:

$$BV(\Omega) = \left\{ f : f \in L^{1}(\Omega), TV(f) < \infty \right\} \tag{9}$$

Banach space is formed by BV  $(\Omega)$  under the following norm:  $\|f\|_{\mathbb{B}^{V}} = \|f\|_{L^{1}} + TV(f)$ .

Three fundamental properties of BV space deserve special attention, which are listed as below:

$$\int_{\Omega} \left| Df \right| \leq \lim \inf_{n \to \infty} \int_{\Omega} \left| Df_n \right|$$

**Property 1: Lower semi-continuity:** If  $f_{n-f}$  in  $L^1(\Omega)$  is of weak convergence, we can get the inequality:

$$\int_{\Omega} |Df| \le \lim \inf_{n \to \infty} \int_{\Omega} |Df_n|$$

**Property 2: Compactness:** BV  $(\Omega) \rightarrow L^1(\Omega)$  is compact, in other words, unit spheres in BV  $(\Omega)$  are rather dense in  $L^1(\Omega)$ .

Property 1 and 2 ensure the existence of the variation solutions to the functional with TV items. The following property will demonstrate that BV space has more advantages over traditional Euclid space.

**Property 3: Co-area:** Per (Q) is introduced to describe the circumference of  $Q \subseteq \Omega$ :

$$Per(Q) = \int_{\Omega} |D1_{Q(x)}| = TV(1_{\Omega})$$
 (10)

where,  $1_Q$  is an indicator function. For a given  $u \in BV(\Omega)$ , Co-area is formulated as follows:

$$\int_{\Omega} |D\mathbf{u}| = \int_{-\infty}^{\infty} \mathbf{Per}(\mathbf{u} < \lambda) d\lambda \tag{11}$$

This equation proves that TV (u) is actually a total sum of length of all the contours related to u.

# HYBRID MODEL USING REGION INFORMATION

The evolution equation of C-V model is given in the Eq. 7. After simplification as,  $\lambda_1 = \lambda_2 = \lambda$ ,  $r(x, c_1, c_2) = (I(x)-c_1)^2-(I(x)-c_2)^2$ , it is formulated as follows:

$$\frac{\partial \phi}{\partial t} = \dot{\mathbf{H}_{\epsilon}}(\phi) \left\{ div \left( \frac{\nabla \phi}{|\nabla \phi|} \right) - \lambda r(\mathbf{x}, \mathbf{c}_1, \mathbf{c}_2) \right\}$$
 (12)

As an approximating function of Heaviside in practical use,  $H_{\epsilon}(\phi)$  is smooth, compactly supported and also strictly monotonic. That means the above formula is equivalent to the following equation in the steady state:

$$\frac{\partial \phi}{\partial t} = \text{div} \left( \frac{\nabla \phi}{|\nabla \phi|} \right) - \lambda r(x, c_1, c_2)$$
 (13)

Moreover, the expression above is precisely a gradient descent flow of an energy function, which can be described as below:

$$E(\phi, \mathbf{c}_1, \mathbf{c}_2, \lambda) = \int_{\Omega} |\nabla \phi| + \lambda \int_{\Omega} \mathbf{r}(\mathbf{x}, \mathbf{c}_1, \mathbf{c}_2) \phi d\mathbf{x}$$
 (14)

where,  $\int_{\Omega} |\nabla \phi|$  is a TV item and  $\phi$  is a level set function. Without being restricted,  $\phi$  tends to be getting close to  $\infty$  due to the evolution of gradient flow. To get valid solutions and keep unanimous with TV, we specify that  $0 \le \phi \le 1$  by using the symbol u:

$$E(\mathbf{u}, \mathbf{c}_1, \mathbf{c}_2, \lambda) = TV(\mathbf{u}) + \lambda \int_{\Omega} \mathbf{r}(\mathbf{x}, \mathbf{c}_1, \mathbf{c}_2) \mathbf{u} d\mathbf{x}$$
 (15)

For the given parameters  $c_1$ ,  $c_2 \in R$ ,  $\lambda \in R_+$ , if u is the minimum of a functional, we can derive an indicator function  $1_{\Omega(u)=(xu(x)>\mu)}(x)$ , which is also a global minimization functional of  $E(u, c_1, c_2, \lambda)$ .

**Proof:** As  $u \in [0, 1]$ , according to the reference (Bresson *et al.*, 2007), the level set expression can be described like this:

$$TV(\mathbf{u}) = \int_{\Omega} |\nabla \mathbf{u}| = \int_{\Omega}^{1} Per(\{\mathbf{x} : \mathbf{u}(\mathbf{x}) > \mu\}; \Omega) d\mu$$
 (16)

The integral of  $r(x, c_1, c_2) = (I(x)-c_1)^2-(I(x)-c_2)^2$  and u can be calculated as follows:

$$\begin{split} & \int_{\Omega} (\mathbf{c}_{1} - \mathbf{I}(\mathbf{x}))^{2} \mathbf{u}(\mathbf{x}) d\mathbf{x} \\ & = \int_{\Omega} (\mathbf{c}_{1} - \mathbf{I}(\mathbf{x}))^{2} \int_{0}^{1} \mathbf{1}_{[0,\mathbf{u}(\mathbf{x})]}(\boldsymbol{\mu}) d\boldsymbol{\mu} d\mathbf{x} \\ & = \int_{0}^{1} \int_{\Omega} (\mathbf{c}_{1} - \mathbf{I}(\mathbf{x}))^{2} \mathbf{1}_{[0,\mathbf{u}(\mathbf{x})]}(\boldsymbol{\mu}) d\mathbf{x} d\boldsymbol{\mu} \\ & = \int_{0}^{1} \int_{\Omega \cap (\mathbf{x},\mathbf{u}(\mathbf{x})) \times \boldsymbol{\mu}} (\mathbf{c}_{1} - \mathbf{I}(\mathbf{x}))^{2} d\mathbf{x} d\boldsymbol{\mu} \end{split} \tag{17}$$

$$\int_{\Omega} (\mathbf{c}_{2} - \mathbf{I}(\mathbf{x}))^{2} \mathbf{u}(\mathbf{x}) d\mathbf{x} 
= \int_{0}^{1} \int_{\Omega \cap (\mathbf{x}: \mathbf{u}(\mathbf{x}) > \mu)} (\mathbf{c}_{2} - \mathbf{I}(\mathbf{x}))^{2} d\mathbf{x} d\mu 
= \mathbf{C} - \int_{0}^{1} \int_{\Omega \cap (\mathbf{x}: \mathbf{u}(\mathbf{x}) > \mu)} (\mathbf{c}_{2} - \mathbf{I}(\mathbf{x}))^{2} d\mathbf{x} d\mu$$
(18)

where,  $C = \int_{\Omega} (c_2 - I(x))^2 dx$  is independent of u.

Suppose  $\Sigma(\mu):=\{x:u(x)>\mu\}$ , where,  $u(x)\in L(\Omega)$ ,  $0\le u(x)\le 1$ , a formula can be derived by combining the above-mentioned parts together. It is described as follows:

$$\begin{split} &\widetilde{E}(\mathbf{u}, \mathbf{c}_1, \mathbf{c}_2, \lambda) \\ &= \int_0^1 \left\{ \begin{split} &\operatorname{Per}(\Sigma(\boldsymbol{\mu}); \Omega) + \lambda \int_{\Sigma(\boldsymbol{\mu})} (\mathbf{c}_1 - \mathbf{I}(\mathbf{x}))^2 \, d\mathbf{x} \\ &+ \lambda \int_{\text{CA}\Sigma(\boldsymbol{\mu})} (\mathbf{c}_2 - \mathbf{I}(\mathbf{x}))^2 \, d\mathbf{x} \end{split} \right\} d\boldsymbol{\mu} - \mathbf{C} \end{split} \tag{19}$$

$$&= \int_0^1 E(\Sigma(\boldsymbol{\mu}), \mathbf{c}_1, \mathbf{c}_2, \lambda) d\boldsymbol{\mu} - \mathbf{C}$$

Equation 19 illustrates that if u(x) is a minimization functional, for  $\mu \in [0, 1]$ ,  $\Sigma(\mu)$  is also a minimization functional of  $E(u, c_1, c_2, \lambda)$ .

As it is shown in equation (1), GAC model is essentially an energy function which describes the weighted length of curves. The weights depend on g (x), which is an edge indicator function. Suppose the restored image u (x) is restricted to a two-valued function that means image restoration is equivalent to its segmentation. Since  $|\nabla l_{\Omega}|$  can be used to denote the edge of the function, we can derive the following:

$$E_{GAC}(C) = \int_{C} g(\mathbf{x}) d\mathbf{s} = \int_{\Omega} g(\mathbf{x}) |\nabla \mathbf{1}_{\Omega}| d\mathbf{x}$$
 (20)

Bresson *et al.* proved the following equation (Bresson *et al.*, 2007):

$$E_{GAC}(C) = TV_{\varepsilon}(u = 1_{\Omega_{\varepsilon}})$$
 (21)

where,  $TV_g(u) = \int_{\Omega} g(x) |\nabla u| d\Omega = |\nabla u|_g$ . This means that the GAC energy is equal to the weighted TV-norm when the function u is a characteristic function of a closed set  $\Omega_c \subset \Omega$ . They also proved that u is almost allowed to vary continuously between [0,1]. The advantage of  $TV_g(u)$  over  $E_{GAC}(C)$  is its (non-strict) convexity and easy to add region information.

In many algorithms, the region information is only used to move the curve to the strong edge. It fails to segment a region in a complex backgroud. We proposed a region term in our model:

$$E_{\rm region}(u) = \int_{\Omega} (1 - 2I_{\rm reg}) u \, d\Omega \tag{22}$$

where,  $I_{\text{reg}}(x) \in \{0, 1\}$ , for  $\forall x \in \Omega$ , is a mask to identify the location information and  $(1\text{-}2I_{\text{reg}}(x)) \in \{\text{-}1, 1\}$ . This term is used to punish the difference between u and  $I_{\text{reg}}$ . Through a combination of  $E_{\text{region}}(u)$  and  $TV_g(u)$ , a novel energy is obtained to assemble edges around a labeled region to get an accurate segmentation. Then the hybrid model can be formulated as follow:

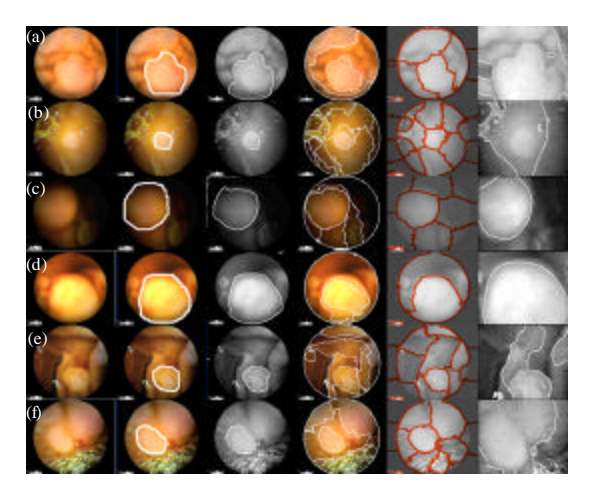


Fig. 1(a-f): Segmentation results of our method in comparison with other four methods. In each row, we present; (a) Original image, (b) The segment results by human expert, (c) The segment results of our method, (d) The segment results of MShift, (e) The segment results of Ncut, (f) The segment results of GGAC

$$\min_{u \in \mathcal{A}} \left\{ E_{seg}(u) = TV_g(u) + \mu E_{region}(u) \right\}$$
 (23)

where,  $\mu$  is an arbitrary positive constant to control the influence of the edge term and the region term. The approaches to solve this model can be seen in our precious study (Liu *et al.*, 2013).

# EXPERIMENTAL RESULTS AND DISCUSSION

To test and evaluate the performance of the proposed segmentation approach for wireless capsule endoscopy images, we compared the proposed method with three state-of-art image segmentation algorithms: the Mean Shift method (MShift) (Comaniciu and Meer, 1997), the normalized cut algorithm (Ncut) (Shi and Malik, 2000) and GGAC. The input of our method and GGAC is intensity image and of MShift and Neut is color image of Lab color space. The parameters of the proposed method are generally chosen as follows:  $\sigma_1 = 2$ ,  $\sigma_2 = 20$ , h = 2,  $\eta = 0.8$ ,  $\kappa = 0.85$ ,  $\mu = 0.01$ ,  $\lambda = 10$ . For MShift which is quite sensitive of the parameter of minimal region area and for Ncut the number of partitions also heavily influence the segment result, we run these methods several times with different parameterization and finally choose the best results to show. Because GGAC is a two-phase segment method, the black background around the circle sense is clipped down as a pre-processing. The experiment results including human labeled segmentations are shown in Fig. 1. It is easy to see that even under such unfair experimental setup, the results of our method visually demonstrated more closely to the human expert outline. It demonstrate that our method performance better than other many different methods (i.e., MShift algorithm, Ncut algorithm and GGAC model) on various kinds of polyp images.

# CONCLUSION

In this study, we proposed a new model to segment wireless capsule endoscopy images which combine edge and region information. The region information is represented by a simple binary mask and the edge information is abstracted from the gradient image. A global optimal total variation model is employed to combine them together. To test and evaluate the proposed approach, a number of experiments have been carried out. Experimental results demonstrate the its efficacy

### ACKNOWLEDGMENT

This study was supported in part by the Industry-Academia Cooperation Innovation Fund Projects of Lianyungang (Grant No. CXY1203) and by the Technology Research and Development Program of Lianyungang (Grant No. SH1223).

# REFERENCES

- Bresson, X., S. Esedoglu, P. Vandergheynst, J.P. Thiran and S. Osher, 2007. Fast global minimization of the active contour/snake model. J. Math. Imaging Vision, 28: 151-167.
- Caselles, V., R. Kimmel and G. Sapiro, 1997. Geodesic active contours. Int. J. Comput. Vision, 22: 61-79.
- Chan, T.F. and J. Shen, 2002. A good image model eases restoration-on the contribution of Rudin-Osher-Fatemi's BV image model. March, 2002. http://www.ima.umn.edu/preprints/feb02/1829.pdf

- Chan, T.F. and L.A. Vese, 2001. Active contours without edges. IEEE Trans. Image Process., 10: 266-277.
- Comaniciu, D. and P. Meer, 1997. Robust analysis of feature spaces: Color image segmentation. Proceedings of the 1997 IEEE Computer Society Conference on Computer Vision and Pattern Recognition, Jun 17-19, 1997, San Juan, pp: 750-755.
- Guliato, D., R.M. Rangayyan, J.A. Zuffo and J.L. Desautels, 1998. Detection of breast tumor boundaries using iso-intensity contours and dynamic thresholding. Digital Mammography, 13: 253-260.
- Kass, M., A. Witkin and D. Terzopoulos, 1988. Snakes: Active contour models. Int. J. Comput. Vision, 1: 321-331.
- Liu, J., J. Liang and Y. Lan, 2013. TV-Seg: Total variation segmentation with imprecise region information. J. Applied Sci., 13: 2102-2106.
- Mendoza, C.S., B. Acha, C. Serrano and T. Gomez-Cha, 2012. Fast parameter-free region growing segmentation with application to surgical planning. Machine Vision Appli., 23: 165-177.
- Petrick, N., H.P. Chan, B. Sahiner and M.A. Helvie, 1999. Combined adaptive enhancement and region-growing segmentation of breast masses on digitized mammograms. Med. Phys., 26: 1642-1654.
- Shi, J. and J. Malik, 1997. Normalized cuts and image segmentation. IEEE Trans. Pattern Anal. Mach. Intell., 22: 888-905.
- Timp, S. and N. Karssemeijer, 2004. A new 2D segmentation method based on dynamic programming applied to computer aided detection in mammography. Med. Phys., 31: 958-971.
- Zhang, Z., C. Chen, J. Sun and K.L. Chan, 2003. EM Algorithms for Gaussian mixtures with split and merge operation. Patt. Recog., 36: 1973-1983.
- Adams, R. and L. Bischof, 1994. seeded region growing. IEEE Transactions on Pattern Analysis and Machine Intelligence 16, 6 (June), 641–647.